International Journal of Applied Engineering Research
ISSN 0973-4562 Volume 10, Number 4 (2015) pp. 9355-9373

http://www.ripublication.com

# Impact of Size and Location of WECS on Power System Eigenvalue Stability Analysis

**[1]Dr S.G. Bharathi Dasan, [2]Dr. R.P.Kumudini Devi and [3]Sharon Ravichandran**
*[1]Associate Professor Department of EEE Sri Venkateswara college of Engineering, Sriperumbudur,Chennai, India*
*[2]Professor[3] Research scholar Department of EEE, College of Engineering, Anna University Chennai, India.*

## Abstract

Large penetration of wind generation would have far reaching consequences on the grid. Before installing wind generators, utility engineers must analyze the worst operating scenarios to guarantee that the power system will not be adversely affected by the wind generators. Basically, synchronous machine rotor is prone to weakly damped (low frequency) oscillations. This work is intended to find the effect of location of wind energy conversion system on small signal stability conditions of conventional power system with synchronous generators (SG). Eigen value analysis is conducted after developing a Differential-Algebraic model (DAE) in power balance form and tested on a modified 3 synchronous machine - 9 bus system with constant speed wind turbines.

**Index Terms:** DG, WECS, SG and EIGENVALUE.

## Introduction

Nomikos & Vournas (2005) investigated power system small-signal stability, considering induction machines as dynamic elements. In this study, a linearized model for a multi-machine system that includes both synchronous and induction machines is presented. Tabesh & Iravani (2006) introduced a small-signal dynamic model of a fixed-frequency induction machine based wind farm connected to an electrical power system. Fernandez et al (2007) dealt with the impact of wind farms on the network frequency dynamics and on its control. Vowles et al (2008) assessed the impact of increasing the amount of wind generation on the damping performance of the New Zealand power system.

Ulianov et al (2008) presented the small signal stability analysis of squirrel cage induction generator with model presented by Kundur (1993). The modeling and simulation is done with Matlab and a toolbox for stability purposes, called PSAT

(Power System Analysis tool box). Li et al (2010) examined the impact of the increased penetration of squirrel cage induction generator based WECS on small signal stability for a single machine infinite system. Yuanzhang et al (2010) provided an overview of recent progresses on the impact of the integration of large amounts of wind power on power system small signal stability and corresponding control strategies to enhance small signal stability. The influence of wind turbine generators on power system damping is analyzed qualitatively by modal analysis and time-domain simulations.

Mendonça & Lopes (2005) dealt with the problem of large wind power integration and its potential impact on systems small signal stability. Hossain et al (2011) investigated critical issues that limit the large-scale integration of wind generators and voltage compensation**.** Rahimi & Mostafa (2009) have analytically investigated the dynamic behaviour of fixed speed wind turbines under wind speed fluctuations .The study of dynamic behaviour included modal and sensitivity analysis, dynamic behaviour analysis under wind speed fluctuation and eigenvalue tracking.

Tohidi et al (2010) describe modeling and small signal analysis of a grid connected fixed speed wind turbine generator. A complete model of FSWECS is derived. Loo et al (2013) presented a mathematical modeling of synchronous and induction generators for wind turbines using state-space representations. Emphasis is given to those models suitable for control schemes of variable-speed wind turbines and their application for different power system studies. The state-space representations provide a convenient way to assess different configurations of fixed and variable-speed wind turbines based on synchronous and induction generators.

The aim of this paper is to simulate the effect of penetration of fixed speed WECS at different locations on Eigenvalues of the power system with SGs. Eigenvalues movement and stability of the system studied for wind velocity changes.

## Small Signal Model of Power System Components

To develop a small signal linear model, the power balance form of the network equations is used. In this formulation, the nonlinear loads are modelled more easily and naturally approach is used for developing linearsied DAE model.

*A. State Space model*

Two axis model of synchronous generator with static exciter is considered. Linearization of DAE power system model is carried out by adopting the concepts presented in [17]. Linearizing the differential equations,

$$\Delta\dot{x} = A_1\Delta x + A_2\Delta I_g + A_3\Delta\hat{V}_g + E\Delta U \quad (1)$$

The stator algebraic equations are linearized as

$$0 = B_1\Delta x + B_2\Delta I_g + B_3\Delta\hat{V}_g \quad (2)$$

The network equations are linearized to obtain

$$0 = C_1 \Delta x + C_2 \Delta I_g + C_3 \Delta \hat{V}_g + C_4 \Delta \hat{V}_l$$

$$0 = D_1 \Delta x + D_2 \Delta I_g + D_3 \Delta \hat{V}_g + D_4 \Delta \hat{V}_l \quad (3)$$

where,

$$\Delta x^T_i = \left[\Delta\omega_i \quad \Delta\delta_i \quad \Delta E'_{qi} \quad \Delta E'_{di} \quad \Delta E_{fdi} \quad \Delta V_{Aux1} \quad \Delta V_{Aux}\right] \qquad \Delta \hat{V}_{gi}^T = \left[\Delta\theta_{gi} \quad \Delta V_{gi}\right]$$

$$\Delta I^T_{gi} = \left[\Delta I_{qi} \quad \Delta I_{di}\right] \qquad \Delta \hat{V}_{li}^T = \left[\Delta\theta_{li} \quad \Delta V_{li}\right]$$

The linearized state model of induction generator explained in [21], is added to the above state space model by defining

$$\Delta x_{IG} = \left[\Delta\omega_r \quad \Delta E'_r \quad \Delta E'_m\right] \quad (4)$$

## Simulation Study

Three machine nine bus system shown in Fig. 1 without WECS is here after termed as "base case" in this thesis. Three synchronous generators in the system are considered with a static exciter. Synchronous generators (SG) are modeled (Two axis model). The number of state variables for each SG is five; therefore there are totally 15 state variables for three SGs. They are ω, δ, $E_q'$, $E_d'$ and $E_{fd}$. The data (Anderson & Fouad 1978) for the test system are given Appendix.

The Eigenvalue analysis is carried out for the base case and the results are presented in Table 1. The test system has 5 complex eigenvalues and 4 real eigenvalues. The zero eigenvalue ($\lambda_6$) is due to the fact that individual machine rotor angles are considered as state variables. The test system in base case is stable as all the eigenvalues are lying in the left half of the s-plane (Pai et al 2004). System has rotor modes $\lambda_{1,2}$ and $\lambda_{3,4}$. From participation factor analysis, it is identified that in the $\lambda_{1,2}$ mode SG3 and SG2 are participating and the in the $\lambda_{3,4}$ mode, SG2 and SG1 are participating.

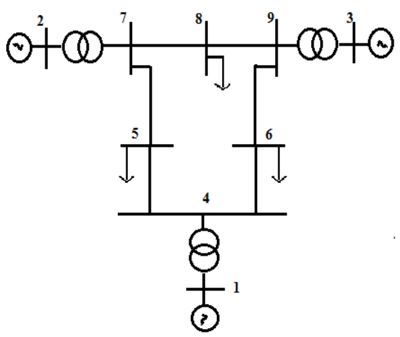


**Figure 1:** Three machines nine bus system

**Table 1:** Eigenvalues of three machine nine bus system without WECS

| Mode | Eigenvalue | State Variables | DR | FR |
|---|---|---|---|---|
| $\lambda_{1,2}$ | -1.4645±12.7670i | $\omega_3$ , $\delta_3$, $\omega_2$ , $\delta_2$ | 0.1140 | 2.0319 |
| $\lambda_{3,4}$ | -0.5183±8.3481i | $\omega_2$ , $\delta_2$ , $\omega_1$ ,$\delta_1$ | 0.0620 | 1.3286 |
| $\lambda_{5,6}$ | -2.2474±3.0219i | $E_{q1}'$ , $E_{fd1}$, $E_{q2}'$ , $E_{fd2}$ | 0.5968 | 0.4810 |
| $\lambda_{7,8}$ | -4.6575±1.4107i | $E_{fd3}$, $E_{d3}'$ , $E_{fd2}$, $E_{d2}'$ | 0.9571 | 0.2245 |
| $\lambda_{9,10}$ | -3.4904±1.0218i | $E_{fd1}$ ,$E_{fd2}$,$E_{d2}$,$E_{q1}$ | 0.9597 | 0.1626 |
| $\lambda_{11}$ | -0.0000 | $\delta_1$, $\delta_2$ ,$\delta_3$ ,$\omega_1$ | 1.0000 | 0.0000 |
| $\lambda_{12}$ | -2.2416 | $E_{q2}'$,$E_{q1}'$ ,$E_{fd2}$, $E_{fd1}$ | 1.0000 | 0.0000 |
| $\lambda_{13}$ | -0.4480 | $\omega_1$ | 1.0000 | 0.0000 |
| $\lambda_{14}$ | -0.8779 | $E_{q3}'$ ,$E_{q2}'$ ,$E_{d3}'$ ,$E_{fd3}$, $E_{fd2}$ | 1.0000 | 0.0000 |
| $\lambda_{15}$ | -3.2258 | $E_{d1}'$ ,$\omega_1$,$\delta_1$,$E_{q1}'$,$E_{fd1}$ | 1.0000 | 0.0000 |

By assuming that system loads are unchanged, squirrel cage induction generator (SCIG) based fixed speed (FS) WECS are placed with/without replacing the existing synchronous generators except slack generator (SG1). The reactive power absorbed by the SCIGs is provided by fixed capacitors. The following cases are considered for the analysis.

- Case 1- WF to replace SG2 with equal capacity.
- Case 2- WF to replace SG3 with equal capacity.
- Case 3- WF connected at 7$^{th}$ bus without replacing SGs.

### B. Case 1- Fixed Speed Wind Farm At Bus 2

In the three machine nine bus system shown in Fig.1, the second synchronous generator is replaced by fixed speed wind farm. The wind farm is represented by an equivalent wind turbine generator by adopting simple aggregation. In simple aggregation it is assumed that all the wind turbine generators are operating at same wind velocity. A third order model is used for IGs. The state variables of IG are slip, $E_r'$ and $E_m'$. The number of state variables for each SG is five; therefore there are totally 13 state variables for the modified test system. Induction generator data is given in Appendix (Lubosny 2003).

The size of the second synchronous generator is 163MVA. A wind farm comprising 180 wind turbine generators with each wind turbine generator rated at 0.9 MW is considered to replace the SG at bus 2. Analyses are carried out for rated wind velocity of 17 m/s.

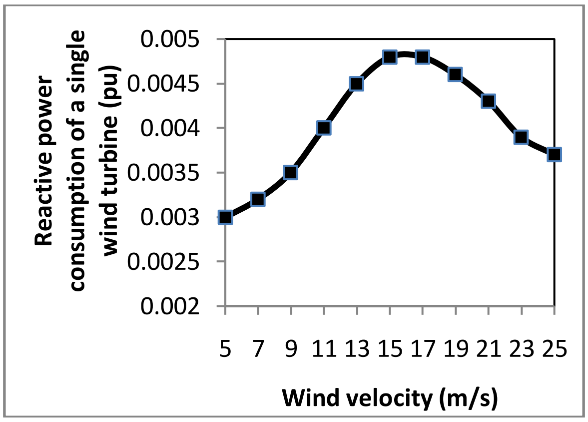


**Figure 2:** Reactive power absorption of simple WTG with wind velocity

Power flow analysis (Jayashri 2007) is conducted by including slip of the induction generator as a state variable. Since it is a fixed speed WECS the range of slip is ± 5%. From Fig. 2 it can be noted that at rated wind velocity of 17 m/s reactive power absorbed by IG is 0.0048pu which is given by capacitors. Initial conditions are calculated from the power flow analysis and then small signal stability analysis is performed. Eigenvalues, damping ratio, frequency of oscillations and state variables participating in each mode are presented in Table 2. A comparison of eigenvalues without and with wind farm at bus 2 is presented in Table 3.The system is stable after the replacement of SG2 with IG.

Since second generator is replaced by IG, rotor mode ($\omega_2$, $\delta_2$) of SG2 would be absent. It can be observed from Table 4.3 that in the rotor mode third and first generator angular speeds and rotor angles ($\omega_3$, $\delta_3$ and $\omega_1$, $\delta_1$) are participating. But IG introduces two electromechanical modes ($\lambda_3$ and $\lambda_{4,5}$). The participation factors corresponding to the modes indicate the contribution of every generator.

**Table 2:** Eigenvalues of three machine nine bus system with FS wind farm at bus2

| Modes | Eigen values | Damping Ratio | Frequency of oscillations (Hz) | State Variables |
|---|---|---|---|---|
| $\lambda_{1,2}$ | -0.9018±8.1408i | 0.1101 | 1.2956 | $\omega_3,\delta_3,\delta_1,\omega_1$ |
| $\lambda_3$ | -8.4435 | 1.0 | 0 | $\omega_{ig}$, $E_m$’ |
| $\lambda_{4,5}$ | -3.3723±3.5200i | 0.6918 | 0.5602 | $E_m$’ ,$\omega_1,\delta_1,\omega_{ig}$ |
| $\lambda_{7,8}$ | -3.9911±2.1548i | 0.8799 | 0.3429 | $E_m$’ , $E_{fd3}$ ,$E_{d3}$’ ,$E_{q3}$’ |
| $\lambda_{9,10}$ | -2.3773±1.8626i | 0.7872 | 0.2964 | $E_{q1}$’ , $E_{fd1}$, $E_m$’ |
| $\lambda_{11,12}$ | -1.7620±0.7017i | 0.9290 | 0.1117 | $E_m$’, $E_r$’ ,$E_{d3}$’ ,$E_{q3}$’ |
| $\lambda_{13}$ | -3.2258 | 1.00 | 0 | $E_{d1}$’ |

**Table 3:** Comparison of eigenvalues without and with FS wind farm at bus 2

| Case | Participation | Eigen value | State Variables | Damping Ratio | Participation factor |
|---|---|---|---|---|---|
| BASE CASE | SG3+SG2 $\lambda_{1,2}$ | -1.4645±12.7670i | $\omega_3$ , $\delta_3$, $\omega_2$ , $\delta_2$ | 0.1140 | 1.00,0.9936, 0.2206,0.219 |
| | SG1+SG2 $\lambda_{5,6}$ | -2.2474±3.0219i | $E_{q1}'$ ,$E_{fd1}$, $E_{q2}'$ ,$E_{fd2}$ | 0.5968 | 1.00,0.9186, 0.7576,0.700 |
| | SG3+SG2 $\lambda_{7,8}$ | -4.6575±1.4107i | $E_{fd3}$, $E_{d3}'$, $E_{fd2}$, $E_{d2}'$ | 0.9571 | 1.00,0.8822, 0.7453,0.706 |
| WITH WIND FARM | SG3+SG1 $\lambda_{1,2}$ | -0.9018±8.1408i | $\omega_3$,$\delta_3$, $\delta_1$,$\omega_1$ | 0.1101 | 1.00,1.00, 0.1655,0.165 |
| | SG1+IG $\lambda_{9,10}$ | -2.3773±1.8626i | $E_{q1}'$ , $E_{fd1}$, $E_m'$, $\omega_1$, $\delta_1$ | 0.7872 | 1.00,0.9082, 0.4818,0.198 |
| | IG+SG3 $\lambda_{7,8}$ | -3.9911±2.1548i | $E_m'$, $E_{fd3}$, $E_{d3}'$ ,$E_{q3}'$ | 0.8799 | 1.00,0.8496, 0.6556,0.468 |

The modes of synchronous generator are compared for with and without wind farm. It is found that SG3 rotor mode damping ratio is decreased by 3.42% with wind farm at bus 2 and SG3 electrical mode ($\lambda_{7,8}$) damping decreases by 8.06%. The participation factor analysis reveals that in SG3 electrical mode, IG electrical variable $E_m'$ is also contributing strongly. Similarly, IG contributes in SG1 electrical mode. But SG1 electrical mode ($\lambda_{9,10}$) damping increases significantly by 31.90%. Small signal stability analysis is conducted by varying wind velocity, number of wind turbines and load at all the busses.

**(i) Impact of Wind Velocity**

Wind is varying in nature. So, small signal stability analysis should be done for different wind velocities. The analysis explained in previous section is repeated for different wind velocities between cut-in (5 m/s) and cut-out (25 m/s). Movement of eigenvalues with respect to wind velocity is presented in Figures 3, 4 and 5.

Fig. 3 shows the movement of two ($\lambda_{1,2}$ and $\lambda_{4,5}$) SG modes. In the $\lambda_{1,2}$ mode, rotor variables of synchronous generators 1 and 3 are participating. This mode moves toward the origin slowly. But in the $\lambda_{4,5}$ mode, along with rotor variables of SG1, electrical state variable of IG, $E_m'$ is also participating due to which eigenvalue shows a wide movement away from the origin to left half of the s-plane for the change in wind velocity.

Fig. 4 shows the movement of two IG modes ($\lambda_{11,\ 12}$ and $\lambda_3$ ). $\lambda_{11,\ 12}$ mode is an electromechanical mode in which state variables $E_m$ and $E_r$ are strongly participating along with small participation of electrical variables of synchronous generator 3. $\lambda_3$ mode is an electromechanical mode in which $\omega_{ig}$ and $E_m$' are participating. Both modes move away from the origin. Particularly, $\lambda_3$ mode shows a wide movement away from the origin for the change in wind velocity. This makes the system more stable.

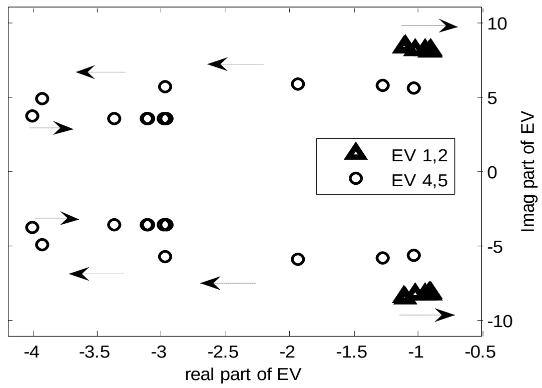


**Figure 3:** SG rotor modes movement with wind velocity-case 1

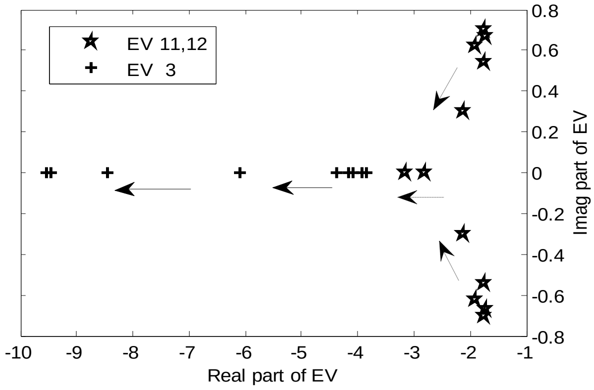


**Figure 4:** IG modes movement with wind velocity-case 1

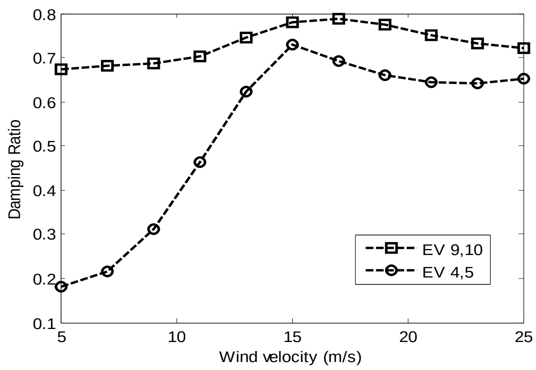


**Figure 5:** Damping ratio of electrical modes ($\lambda_{9,10}$ and $\lambda_{4,5}$) with wind velocity-case 1

Fig. 5 reveals that the damping ratios of $\lambda_{9,\ 10}$ and $\lambda_{4,\ 5}$ modes increase with wind velocity. The conclusions that can be made are (a) all IG modes are moving away from origin (b) SG3 rotor mode moves toward the origin and (c) damping ratio increases for electrical modes of both IG and SG.

**(ii) Impact of the Number of Wind Turbines**

This section presents the impact of varying the size of the wind farm on small signal stability analysis of power system. The performance of the power system is affected with respect to the location and penetration of WECS. In this section number of wind turbines is varied from minimum to the maximum number (180) required for replacement of SG2.

Movement of SG and IG modes with respect to number of turbines is shown Figures 6, 7 and 8. From Fig. 6 it is found that $\lambda_{4,5}$ mode is moving towards the origin. In this electromechanical mode, IG Electrical variable $E_m$' is strongly participating along with the participation of rotor variables of SG1 and IG. On the other hand, SG rotor mode ($\lambda_{1,2}$) and IG electrical mode ($\lambda_{11,12}$) become stronger with change in number of wind turbines which is shown in Fig. 7.

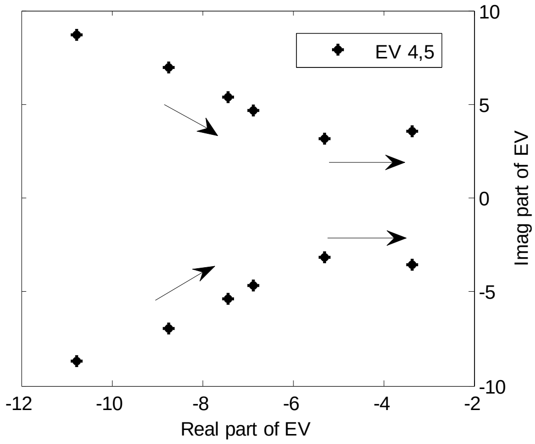


**Figure 6:** IG electromechanical mode movement with number of turbines- case 1

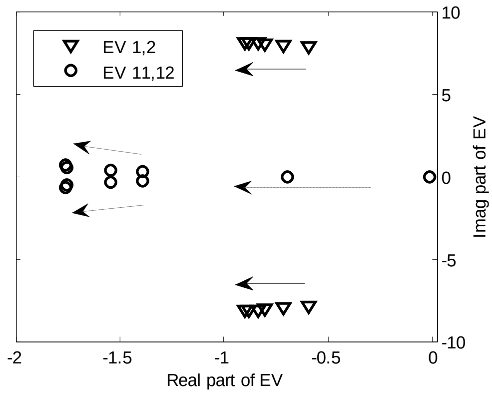


**Figure 7:** SG rotor modes movement with number of turbines-case 1

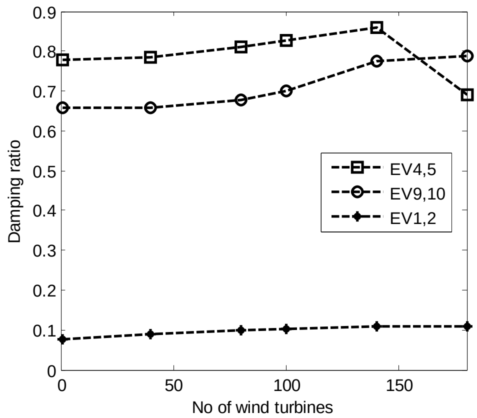


**Figure 8:** Effect of increasing wind penetration on damping ratio of $\lambda_{4,5}$ , $\lambda_{9,10}$ and $\lambda_{1,2}$ modes-case 1

Fig. 8 reveals that slight increase in damping ratio of SG1 electrical mode ($\lambda_{9,10}$) , SG3 rotor mode($\lambda_{1,2}$) and IG electromechanical mode ($\lambda_{4,5}$) is achieved with increase in number of turbines. The variations shown are up to 180 turbines.

**(iii) Time Domain Analysis**

Eigen value analysis reveals that test system is stable while replacing SG2 by fixed speed wind farm of equal capacity. The change of velocity profile also yields a stable performance. The results of eigenvalues analysis are validated with time-domain simulations. The wind velocity is increased by 10% from its rated velocity at 1 second. The relative load angle, real power generation and bus voltages of synchronous generators and slip, real power generation and bus voltage of fixed speed WF are studied. Fig. 9 presents the slip, real power and voltages of wind farm at bus 2. Fig. 10 depicts relative angle, the real powers and bus voltages of SG1 and SG3.

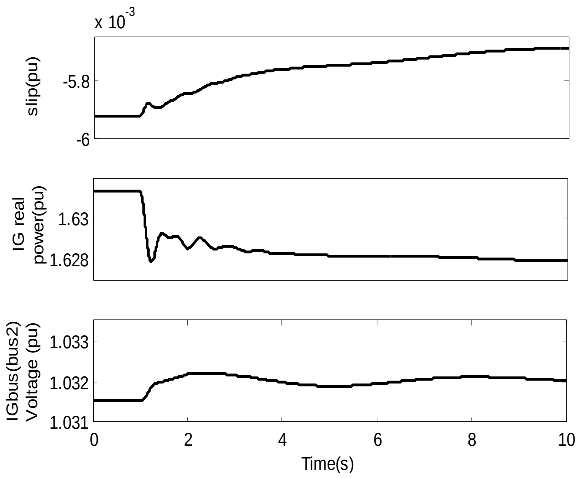


**Figure 9:** Responses of (a) Slip (b) IG real power (c) Bus 2 voltage for step change in wind velocity-case 1

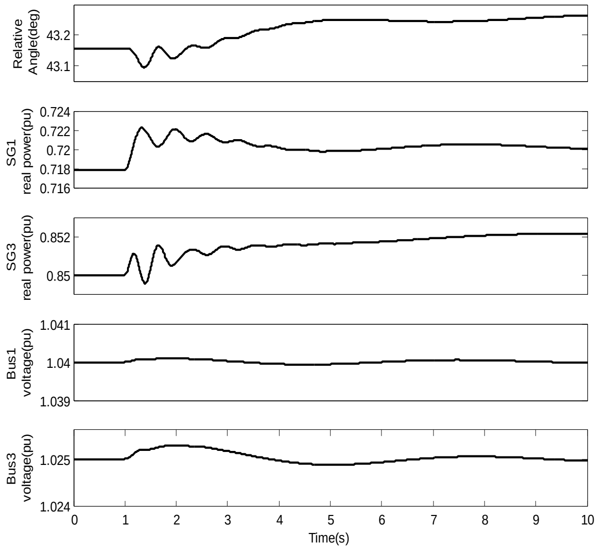


**Figure 10:** Responses of (a) Relative angle (SG1-SG3) (b) SG1 real power (c) SG3 real power (d) Bus 1 voltage and (e) Bus 3 voltage for step change in wind velocity-case 1

It is observed from the Figures, that when wind velocity is increased by 10% the real power output starts decreasing with decreasing negative slip. Slip is settled at the new value, -0.0057p.u. This is due to the narrow band slip operation of fixed speed WECS. The voltage at bus 2 increases from 1.0316 pu to 1.0322pu. Fig. 10 presents the effect of change in wind velocity on SG1 and SG3. The real power output of SGs increase to compensate the decrease in real power generation of wind farm at bus 2. The voltage of SGs is also affected by the disturbance. All the variables settle down to a new operating point after the disturbance. However, system stability is maintained.

### C. Case 2 – Fixed Speed Wind Farm At Bus 7

**Table 4:** Eigenvalues of three machine nine bus system with FS wind farm at bus 7

| Modes | Eigenvalues | Damping ratio | Frequency of Oscillations | State variables |
|---|---|---|---|---|
| $\lambda_{1,2}$ | -0.9520±11.8361i | 0.0802 | 1.8838 | $\omega_3,\delta_3,\omega_2,\delta_2$ |
| $\lambda_{3,4}$ | -2.4562 ± 9.3935i | 0.2530 | 1.4950 | $\omega_2,\delta_2,E_r',E_m'$ |
| $\lambda_5$ | -8.7956 | 1.0000 | 0.0000 | $\omega_{ig},E_m',E_r'$ |
| $\lambda_{6,7}$ | -2.9556 ± 3.7582i | 0.6182 | 0.5981 | $E_m',\omega_1,\delta_1$ |
| $\lambda_{8,9}$ | -0.6179 ±1.9293i | 0.3050 | 0.3071 | $E_r'$, $E_m'$, $\omega_1,\delta_1$ |
| $\lambda_{11,12}$ | -5.0619±1.1124i | 0.9767 | 0.1771 | $E_{d2},E_{fd2}$ |
| $\lambda_{13,14}$ | -3.7197±1.7515i | 0.9047 | 0.2788 | $E_{fd3},E_{d3'},E_{q3'}$ |
| $\lambda_{15,16}$ | -2.4191±1.6238i | 0.8303 | 0.2584 | $E_{q1}',E_{fd1}$ |
| $\lambda_{17}$ | -1.6460 | 1.0000 | 0.0000 | $E_{q3}',E_{d3}',E_{fd3}$ |
| $\lambda_{18}$ | -3.2258 | 1.0000 | 0.0000 | $E_{d1}'$ |

**Table 5:** Comparison of eigenvalues without and with FS wind farm at bus 7

| Case | Modes | Eigenvalue | State Variables | Damping Ratio |
|---|---|---|---|---|
| BASE CASE | $\lambda_{1,2}$ SG3+SG2 | -1.4645±12.7670i | $\omega_3$ , $\delta_3$, $\omega_2$ , $\delta_2$ | 0.1140 |
| | $\lambda_{3,4}$ SG2+SG1 | -0.5183±8.3481i | $\omega_2$ , $\delta_2$ , $\omega_1$ ,$\delta_1$ | 0.0620 |
| | $\lambda_{5,6}$ SG1+SG2 | -2.2474±3.0219i | $E_{q1}$',$E_{fd1}$, $E_{q2}$',$E_{fd2}$ | 0.5968 |
| | $\lambda_{7,8}$ SG3+SG2 | -4.6575±1.4107i | $E_{fd3}$, $E_{d3'}$, $E_{fd2}$, $E_{d2'}$ | 0.9571 |
| | $\lambda_{9,10}$ SG1+SG2 | -3.4904±1.0218i | $E_{fd1}$,$E_{fd2,}$ $E_{d2}$,$E_{q1}$ | 0.9597 |
| WITH WIND FARM | $\lambda_{1,2}$ SG3+SG2 | -0.9520±11.8361i | $\omega_3$,$\delta_3$, $\omega_2$,$\delta_2$ | 0.0802 |
| | $\lambda_{3,4}$ SG2+IG | -2.4562 ± 9.3935i | $\omega_2$,$\delta_2$, $E_r$',$E_m$' | 0.2530 |
| | $\lambda_{15,16}$ SG1 | -2.4191±1.6238i | $E_{q1}$',$E_{fd1}$ | 0.8303 |
| | $\lambda_{13,14}$ SG3 | -3.7197±1.7515i | $E_{fd3}$,$E_{d3}$', $E_{q3}$ | 0.9047 |
| | $\lambda_{11,12}$ SG2 | -5.0619±1.1124i | $E_{d2}$,$E_{fd2}$ | 0.9767 |

In three machine nine bus system shown in Fig. 1, without replacing synchronous generators, a fixed speed wind farm is connected as fourth generator at 7$^{th}$ bus and small signal stability of the system is analyzed. There are totally 18 state variables for the modified test system.

From the load flow analysis, it is found that fixed speed wind farm at 7$^{th}$ bus can be a wind farm with maximum of 340 wind turbines. Analyses are carried out for rated wind velocity of 17 m/s. From Table 4, it is identified that the system is stable after the addition of wind farm at 7$^{th}$ bus. It is identified that the third generator rotor mode ($\omega_3$, $\delta_3$ and $\omega_2$, $\delta_2$) remain combined with second generator mode ($\lambda_{1,2}$) as in base case. But second generator rotor mode and first generator rotor mode is individually combined with electrical variables of IG ($\lambda_{3,4}$ and $\lambda_{6,7}$ respectively).

The modes of synchronous generator are compared for with/without WECS cases in Table 5. It is found that SG3 rotor mode ($\lambda_{1,\,2}$) damping is decreased by 29.65% and SG2 rotor mode ($\lambda_{3,4}$) damping increases three times than in base case. The electrical modes of SGs in base case $\lambda_{5,6}$ , $\lambda_{7,8}$ and $\lambda_{9,10}$ show the significant change while adding wind turbine at 7th bus. Mode $\lambda_{15,16}$ attains 39.125% increase in damping than its counterpart $\lambda_{5,6}$ in base case. Mode $\lambda_{11,12}$ attains 1.77% increase in damping than its counterpart $\lambda_{9,10}$ in base case. But mode $\lambda_{7,8}$ damping decreases by 5.47% ($\lambda_{13,14}$ in case 2). As a conclusion, providing fixed speed wind farms increases damping of SG rotor modes compared to base case. Eigenvalues are studied by varying wind velocity and by varying number of wind turbines in this section.

**(i) Impact of Wind Velocity**

The analysis is repeated for different wind velocities between cut-in (5 m/s) and cut-out (25 m/s). Fig. 11 shows the movement of $\lambda_{1,2}$, $\lambda_{3,4}$ and $\lambda_{6,7}$ rotor modes they move away from the origin. The arrow mark shows the increasing direction of wind velocity. Around rated wind velocity, $\lambda_{3,4}$ and $\lambda_{6,7}$ move slowly from the origin, but this movement is less compared to initial movement towards the origin.

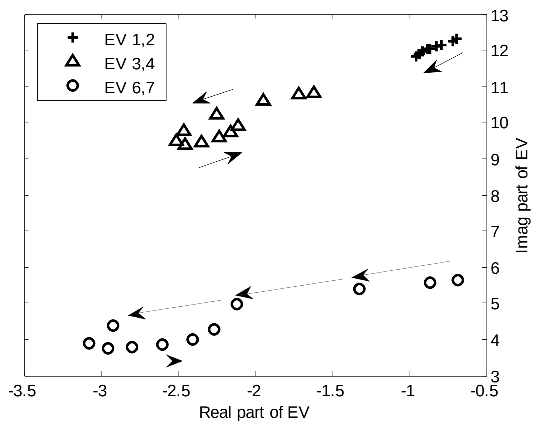


**Figure 11:** SG rotor modes movement with wind velocity-case 2

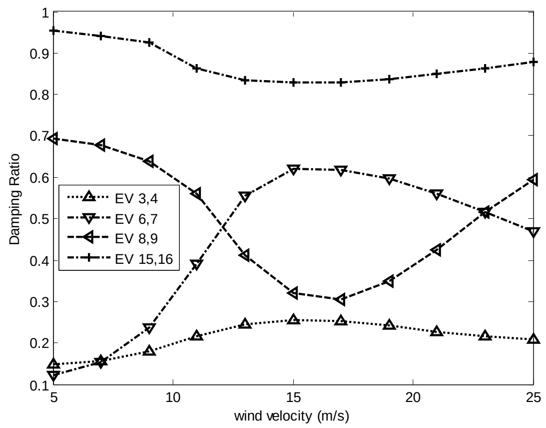


**Figure 12:** Damping ratio of modes with wind velocity-case 2

Fig. 12 shows the changes in damping ratio with wind velocity. Damping ratio of $\lambda_{3,4}$, $\lambda_{6,7}$, $\lambda_{8,9}$ and $\lambda_{15,16}$ modes are plotted with respect to wind velocities. SG2 rotor mode are combined with electrical variables ($E_r$' and $E_m$') of IG in $\lambda_{3,4}$ and SG1 rotor mode is combined with electrical state variable ($E_m$') of IG in $\lambda_{6,7}$. These two modes experience an increase in damping ratio with increase in wind velocity. In $\lambda_{8,9}$ and $\lambda_{15,16}$ modes, electrical variables of IG and SG1 are participating respectively. These two modes experience a decrease in damping ratio with increase in wind velocity.

**(ii) Impact of Number of Wind Turbines**

Similar to case 1, in this section, number of wind turbines is varied from minimum to the maximum number (340 (obtained from load flow analysis) that can be connected at 7$^{th}$ bus. From Fig.13 it is found that SG rotor modes ($\lambda_{3,4}$ and $\lambda_{1,2}$) are moving away from the origin. The arrow mark direction indicates the increase in number of turbines. SG2 rotor mode ($\lambda_{3,4}$) and SG3 rotor mode ($\lambda_{1,2}$) become stronger with change in number of wind turbines. Fig. 14 reveals the increase in damping ratio of $\lambda_{1,2}$, $\lambda_{3,4}$, $\lambda_{13,14}$ and $\lambda_{15,16}$ modes while number of turbines increases.

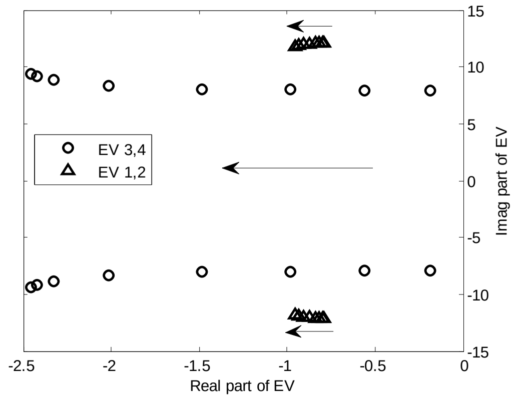


**Figure 13:** SG rotor modes movement with number of wind turbines-case 2

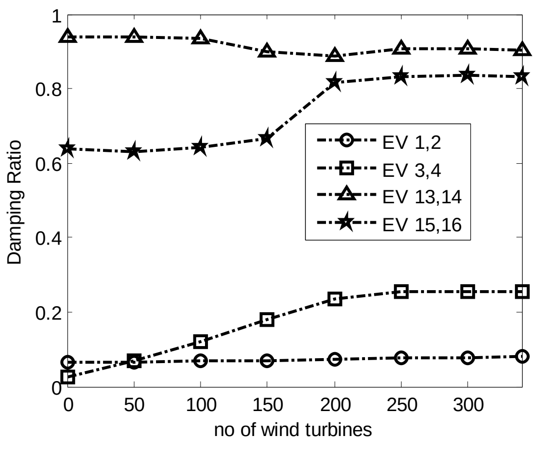


**Figure 14:** Damping ratio of modes with number of wind turbines-case2

**(iii) Time Domain Analysis**

A step increase of 10% is applied at one second from rated wind velocity and the output responses of synchronous generators and fixed speed wind farm are studied as explained in previous section. Fig. 15 depicts the slip, real power and voltage of induction generator at bus 7.

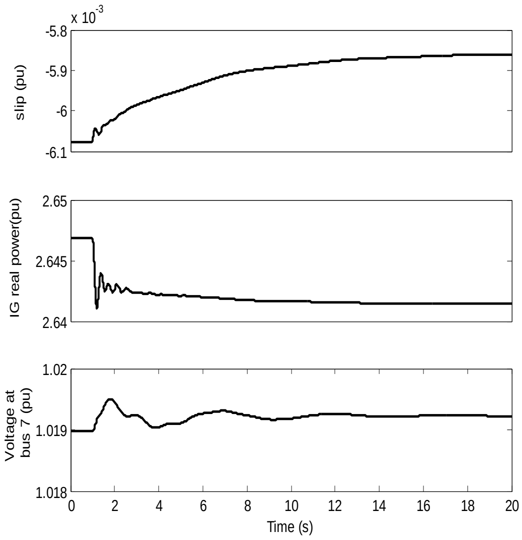


**Figure 15:** Responses of (a) Slip (b) IG real power (c) Bus 7 voltage for step change in wind velocity-case 2

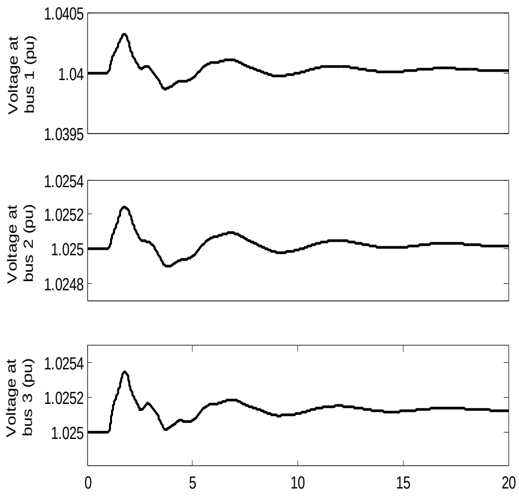


**Figure 16:** Responses of (a) SG1 bus voltage (b) SG2 bus voltage (c) SG3 bus voltage for step change in wind velocity-case 2

Fig. 16 presents the voltage profile at SG buses. It is observed from the figures that when wind velocity is increased by 10% from rated wind velocity, the real power output starts decreasing with decreasing negative slip. Slip is settled at the new value, -0.005863 p.u. This is due to the narrow band slip operation of fixed speed WECS. The voltage at IG bus voltage increases from 1.019 pu to 1.0195pu. The real power output of SGs increase to compensate the decrease in real power generation of wind farm at bus 7.

The voltage of SGs is also affected by the disturbance. All the variables settle down at a new operating point after the disturbance. This is because Type-1 wind turbines do not have any controllers. However, the system is stable.

## Conclusion

Table 6 presents the comparison of salient points while providing fixed speed WECS at three different locations- 2nd bus, 3rd bus or 7th bus. The size of the third synchronous generator is 85 MVA. A wind farm comprising 94 wind turbine generators with each wind turbine generator rated at 0.9 MW is considered to replace the SG at bus 3. The analysis is not presented here in detail by taking the length of paper into account.

**Table 6:** Overall comparison-FSWECS at different locations

| Serial no | Items | FSWECS at bus2 | FSWECS at bus 3 | FSWECS at bus7 |
|---|---|---|---|---|
| 1 | No of turbines and power injected | 180 and 163.2 MW | 94 and 85.22 MW | 340 and 308.41 MW |
| 2 | Fixed capacitor added per turbine | -0.29 MVAR | -0.31 MVAR | -0.48MVAR |
| 3 | Total compensation required | -52.2 MVAR | -29.14 MVAR | -163.2MVAR |
| 4 | Voltage at PCC | 1.0232pu | 1.0311pu | 0.9923pu |
| 5 | Power at bus 1 | 71.46 MW | 71.41 MW | -193.29 MW |
| 6 | Number of EV and state variables | 13 | 13 | 18 |
| 7 | EV closer to origin(real < -1) | 1 | 1 | 2 |
| 8 | Overall damping | -36.4784 | -39.0912 | -50.0321 |
| 9 | No of complex and real modes | 5 and 2 | 5 and 2 | 7 and 3 |

The following conclusions are derived from the above analysis.

1. In this paper, the effect of penetration of fixed speed wind farms is analyzed at three locations (2$^{nd}$, 3$^{rd}$ and 7$^{th}$ bus) in the first part. From small signal stability analysis it is found that providing wind farms at 7$^{th}$ bus is a better choice due to the following reasons.
   a) Eigenvalues closer to the origin in the base case is moved away from the origin in case 3 in comparison with case 1 and case 2. So thereby, system becomes more stable.
   b) Number of turbines that can be connected at 7$^{th}$ bus is high compared to 2$^{nd}$ and 3$^{rd}$ buses.
   c) Overall system damping (31.8498) is increased compared to other two locations (2$^{nd}$ and 3$^{rd}$ buses) (24.0738 and 21.638).
2. The overall effect of SCIG based fixed speed WECS on SGs is positive. SG1 electrical mode damping increases significantly by 31.90% and 8.89% for the cases SG2 replacement and SG3 replacement respectively whereas decrease in damping of other modes is not significant. So overall system stability is improved.
3. During increase in wind velocity, all IG modes make system comfortably stable by moving away from origin with improved damping ratio. Since right movement of SG rotor modes is very minimum compared to left movement of IG modes, it can be concluded that high wind velocity (near to rated value) makes system more stable. When SG2 & SG3 are replaced with IGs, all rotor modes are moving to the left.
4. SG modes become stronger with more number of wind turbines connected in Wind farms. It increases the damping ratio of IG rotor modes and electrical modes of SG.

## Appendix

**A1 Bus Data**

| Bus No | Type | $P_g$ (p.u) | $P_D$ (p.u) | $Q_D$ (p.u) | V (p.u) | $Q_{max}$ (p.u) | $Q_{min}$ (p.u) |
|---|---|---|---|---|---|---|---|
| 1 | 1 | - | - | - | 1.04 | 1 | -1 |
| 2 | 2 | 1.63 | - | - | 1.025 | 1 | -1 |
| 3 | 2 | 0.85 | - | - | 1.025 | 1 | -1 |
| 4 | 3 | - | 0 | 0 | - | - | - |
| 5 | 3 | - | 1.25 | 0.5 | - | - | - |
| 6 | 3 | - | 0.9 | 0.3 | - | - | - |
| 7 | 3 | - | 0 | 0 | - | - | - |
| 8 | 3 | - | 1.0 | 0 | - | - | - |
| 9 | 3 | - | 2.0 | 0.35 | - | - | - |

Type 1-Slack Bus; Type 2-PV Bus; Type 3-PQ Bus

### A2 Transformer And Line Data

| Line | R(p.u) | X(p.u) | B(p.u) | kV |
|---|---|---|---|---|
| 4-5 | 0.01 | 0.085 | 0.088*2 | 230 |
| 4-6 | 0.017 | 0.092 | 0.079*2 | 230 |
| 5-7 | 0.032 | 0.161 | 0.153*2 | 230 |
| 6-9 | 0.039 | 0.17 | 0.0745*2 | 230 |
| 7-8 | 0.0085 | 0.072 | 0.0745*2 | 230 |
| 8-9 | 0.0119 | 0.1008 | 0.1045*2 | 230 |
| 1-4 | 0 | 0.05760 | - | 16.5/230 |
| 2-7 | 0 | 0.06250 | - | 18/230 |
| 3-9 | 0 | 0.05860 | - | 13.8/230 |

### A3 Exciter

$K_A$= [20 20 20] $T_A$=[0.2 0.2 0.2]sec

### A.4 Wind Generator Data

Gear box ratio - 67.5 Blade radius - 26.1m Pitch angle – 4 degree

### A.5 Power Coefficients

$C_1 = 0.5$ $C_4 = 0$ $C_2 = 67.56$ $C_5 = 1.517$ $C_3 = 0$ $C_6 = 16.286$

### A.6 Induction Generator Data

R1=0.0034 ohm R2=0.003 ohm X1=0.055 ohm
X2=0.042 ohm Xo=1.6 ohm

## References

.

[1] B. M. Nomikos and C. D. Vournas, "Investigation of Induction Machine Contribution to Power System Oscillations", *IEEE Trans. Power Systems 2005*, vol. 20,pp.916-925.

[2] R.D. Fernandeza, R.J. Mantza, P.E. Battaiottoa, "Impact of wind farms on a power system.An eigenvalue analysis approach" Renewable Energy, Volume 32, 2007 Issue 10, pp 1676-1688.

[3] Mendonça, A & Lopes, JAP 2005, 'Impact of large scale wind power integration on small signal stability', Published in International Conference on Future Power Systems, 2005 at Amsterdam, pp.1-5.

[4] AhmadrezaTabeshand Reza Iravani, "Small-Signal Dynamic Model and Analysis of a Fixed-Speed Wind Farm—A Frequency Response Approach", *IEEE Trans. Power Delivery 2006,* vol. 21,pp.778-787.

[5] D.J. Vowles, Samarasinghe M.J. Gibbard and G. Ancell, "Effect of Wind Generation on Small-Signal Stability - A New Zealand Example"

Power and Energy Society General Meeting Conversion and Delivery of Electrical Energy in the 21st Century, 2008 IEEE.

[6] Ulianov,Y, Jose, L & Navarro, AD2008,Small signal stability analysis of wind turbines with squirrel cage induction generators,Transmission and Distribution Conference and Exposition: Latin America, IEEE/PES.

[7] Li, L, Liangliang, S, Yihan, Y, Youzhong, M & Tao, W 2010, 'Impact of SVC on Small Signal Stability of Induction Generator Connected Power Systems', IEEE Conference.

[8] Yuanzhang, S, Lixin, W, Guojie, L & Jin, L 2010, 'A Review on Analysis and Control of Small Signal Stability of Power Systems with Large Scale Integration of Wind Power', International Conference on Power System Technology, pp.1-6.

[9] Hossain, MJ, Pota, HR Mahmud, MA & Ramos, RA 2011, 'Impacts of Large-Scale Wind Generators Penetration on the Voltage Stability of Power Systems', published in Power and Energy Society General Meeting, IEEE at San Diego, CA, pp.1-8.

[10] Mohsen Rahimi andMostafa Parniani , "Dynamic behavior and transient stability analysis of fixed speed wind turbines" Renewable Energy Volume 34, Issue 12, December 2009, pp 2613-2624 .

[11] Rosas, P 2003, 'Dynamic influences of wind power on the power system. Ph.D. thesis', Technical University of Denmark.

[12] Vestas 2006, V80-1.8 mw datasheet portland, or: Vestas americas. Tech. rep.

[13] Burnham, DJ, Santoso, S&Muljadi, E 2009, 'Variable rotor-resistance control of wind turbine generators' published in Power & Energy Society General Meeting, PES '09. IEEE at Calgary, pp.1-6.

[14] Tohidi, S, Rabiee, A&Parniani, M 2010, 'Influence of Model Simplifications and Parameters on Dynamic Performance of Grid Connected Fixed Speed Wind Turbines', Published in proceedings of international Conference on Electrical Machines - ICEM 2010 at Rome, pp.1-6.

[15] Shawon, MH, AlDurra, A&Muyeen, SM 2012, 'Small signal stability analysis of fixed speed wind generator including SDBR', published in proceedings of international conference on Electrical Machines (ICEM), at Marseille, pp.2165 - 2171.

[16] Loo, UCE, Ekanayake, JB & Jenkins, N 2013, 'State-Space Modeling of Wind Turbine Generators for Power System Studies', IEEE transactions on Industry Applications, vol. 49, no. 1, pp.223-232.

[17] M.A Pai, D.P Sen Gupta, K R Padiyar "Small Signal Analysis of Power Systems", Narosa Publishing House, New Delhi ,2004.

[18] Z.Lubosny,*WindTurbineOperationinElectricPower Systems-Advancedmodelling*,SpringeVerlag,2003

[19] R.Jayashri, "Analysis and performance enhancement of Grid connected Wind Energy Conversion System" Ph.D thesis, Anna University, Chennai, November 2007.

[20] Moharana, A &Varma, R 2011, 'Subsynchronous resonance in single-cage self-excited induction generator based wind farm to series-compensated lines', IET Gener. Transm. Distrib., vol. 5, no. 12, pp.1221-1232.

[21] Kundur, P 1993, 'Power System Stability and Control', McGraw-Hill, inc.

[22] Anderson, PM and Fouad, AA 1978, 'Power System Control and Stability', Iowa State University Press, Ames, Iowa.